Article

Not peer-reviewed version

A Novel Anti-Glypican-3 Monoclonal Antibody G_3Mab-25 for Flow Cytometry, Western Blotting, and Immunohistochemistry

Saori Okuno , Hiroyuki Suzuki , Mika K Kaneko , Yukinari Kato *

Posted Date: 28 October 2025

doi: 10.20944/preprints202510.2209.v1

Keywords: Glypican-3; monoclonal antibody; Cell-Based Immunization and Screening; flow cytometry; immunohistochemistry

 doi:10.20944/preprints202510.2209.v1

Article

A Novel Anti-Glypican-3 Monoclonal Antibody G3Mab-25 for Flow Cytometry, Western Blotting, and Immunohistochemistry

Saori Okuno, Hiroyuki Suzuki, Mika K. Kaneko and Yukinari Kato *

Department of Antibody Drug Development, Tohoku University Graduate School of Medicine, 2-1 Seiryo-machi, Aoba-ku, Sendai, Miyagi 980-8575, Japan.

* Correspondence: yukinari.kato.e6@tohoku.ac.jp (Y.K); Tel.: +81-22-717-8207

Abstract

Glypican-3 (GPC3) belongs to the glypican family of heparan sulfate proteoglycans and is frequently overexpressed in hepatocellular carcinoma (HCC). The overexpression of GPC3 is associated with the poor clinical outcomes, suggesting its potential as a clinically relevant biomarker and therapeutic target. Therefore, anti-GPC3 monoclonal antibodies (mAbs) have been developed in various modalities for tumor diagnosis and therapy. In this study, more than 80 clones of novel anti-GPC3 mAbs were established using a flow cytometry-based high-throughput screening, the Cell-Based Immunization and Screening (CBIS) method. Among them, a clone G3Mab-25 (IgG1, κ) recognized GPC3-overexpressed Chinese hamster ovary-K1 (CHO/GPC3) but not parental CHO-K1 in flow cytometry. Furthermore, G3Mab-25 recognizes endogenous GPC3 in GPC3-expressing HCC cell lines, including HepG2, HuH-7, and JHH-5. G3Mab-25 specifically recognized only CHO/GPC3, but not other GPC family-overexpressed CHO-K1. The dissociation constant values of G3Mab-25 for CHO/GPC3 and HuH-7 were determined to be 1.8×10^{-8} M and 3.9×10^{-9} M, respectively. Moreover, G3Mab-25 detects the N-terminal fragment of GPC3 in western blotting. In immunohistochemistry, G3Mab-25 showed a diverse staining pattern for GPC3 in HCC tissues. G3Mab-25, established by the CBIS method, is a versatile mAb for basic research and is expected to contribute to tumor diagnosis and therapy.

Keywords: Glypican-3; monoclonal antibody; Cell-Based Immunization and Screening; flow cytometry; immunohistochemistry

1. Introduction

Glypican-3 (GPC3) belongs to the glypican family of heparan sulfate proteoglycans and is tethered to the plasma membrane through a glycosylphosphatidylinositol (GPI) anchor [1–3]. GPC3 is a ~70 kDa protein that undergo endoproteolytic cleavage by Furin at the Arg358- Ser359 position, generating a 40 kDa N-terminal fragment and a 30 kDa C-terminal fragment bearing heparan sulfate (HS)–type glycosaminoglycan side chains [4–6]. The N- and C- subunits are covalently linked via disulfide bonds formed by highly conserved cysteine residues [7]. The mature glypican can be released from the cell surface through cleavage of the GPI anchor by the lipase Notum [2,3].

GPC3 expression is tightly regulated in a stage- and tissue-specific manner during development, with high transcript levels detected in fetal liver, lung, and kidney, but absent in most adult tissues [3,8,9]. GPC3 modulates embryonic development by regulating key signaling cascades such as Hedgehog (HH), Wnt, fibroblast growth factor, and bone morphogenetic protein pathways [9–14]. In adult tissues, nonpathological re-expression of GPC3 has been reported in regenerating liver following partial hepatectomy, where it promotes parenchymal regeneration through activation of the HH signaling pathway [15,16]. Furthermore, GPC3 is frequently overexpressed in hepatocellular carcinoma (HCC). The overexpression is associated with undifferentiated, more aggressive HCC and

 doi:10.20944/preprints202510.2209.v1

poor clinical outcomes, suggesting its potential as a clinically relevant biomarker and therapeutic target in HCC [17].

Soluble GPC3 (sGPC3), generated by enzymatic cleavage of GPC-3, is detectable in the serum of HCC patients but undetectable in that of hepatitis patients and healthy individuals [18–20], making it a valuable diagnostic marker in HCC [21,22]. Using monoclonal antibodies (mAbs) against the N-terminal fragment of GPC3, sGPC3 was shown to be superior to α-fetoprotein in sensitivity, and the combination measurement increased overall sensitivity in well- or moderately-differentiated HCC, suggesting that sGPC3 is a serological marker essential for the early detection of HCC [18].

Codrituzumab (derived from mouse anti-GPC3 mAb clone GC33) recognizes the C-terminal fragment (amino acids 524–563) of GPC3 [23]. Codrituzumab induced tumor cell death through antibody-dependent cellular cytotoxicity (ADCC) [23,24] and exhibited antitumor efficacy in preclinical human tumor xenograft models [25]. Furthermore, codrituzumab was evaluated in phase I and II clinical trials for HCC. Despite demonstrating favorable tolerability, these studies did not reveal significant therapeutic efficacy [26,27]. Codrituzumab was further investigated in phase I clinical trials for pediatric solid tumors, including hepatoblastoma, where it has shown good tolerability with minimal toxicity [28]. However, the monotherapy targeting GPC3 is unlikely to achieve sufficient antitumor efficacy [29].

Biodistribution, tumor targeting, and pharmacokinetics of radiolabeled codrituzumab with iodine-124 (^{124}I) were assessed using positron emission tomography (PET) imaging, which demonstrated favorable pharmacokinetics and tumor uptake in HCC patients [30,31]. For radioimmunotherapy, GC33 conjugated with the alpha-emitting radionuclide actinium-225 (^{225}Ac) through the chelator macropa has been evaluated in a preclinical study [32].

GC33 has been developed as a chimeric antigen receptor (CAR) T cell therapy [33]. However, the therapeutic efficacy of CAR T cells in patients with solid tumors has been constrained by the immunosuppressive nature of the tumor microenvironment (TME) [34,35]. The TME not only provides inhibitory signals that attenuate antitumor immune responses but also lacks essential supportive elements, such as cytokines—particularly interleukin-15 (IL-15)—that are critical for the persistence and optimal functionality of tumor-specific T cells. Recently, GC33-based CAR T co-expressing IL-15 increases the expansion, survival in tumors, and antitumor activity in patients with liver cancers [36]. Therefore, the development of anti-GPC3 mAbs is essential for the tumor diagnosis and therapy.

The Cell-Based Immunization and Screening (CBIS) method includes immunizing antigen-overexpressed cells and flow cytometry-mediated high-throughput screening. Using the CBIS method, we have developed various mAbs against membrane proteins including receptor tyrosine kinases [37,38], and chemokine receptors [39,40]. MAbs obtained by the CBIS method possess a variety of epitopes, including conformational epitopes, linear epitopes, and glyco-epitopes, and are suitable for flow cytometry. Furthermore, some of these mAbs are also suitable for western blotting and immunohistochemistry (IHC). This study employed the CBIS method to develop highly versatile anti-GPC3 mAbs.

2. Materials and Methods

2.1. Cell Lines

Mouse myeloma P3X63Ag8U.1 (P3U1), Chinese hamster ovary (CHO)-K1, and human glioblastoma LN229 were obtained from American Type Culture Collection (ATCC, Manassas, VA, USA). Human HCC cell lines, HepG2 and HuH-7, were obtained from the Cell Resource Center at Tohoku University (Miyagi, Japan). Another HCC cell line, JHH-5, was obtained from the Japanese Collection of Research Bioresources (Osaka, Japan).

JHH-5 was maintained in Williams' E medium (Sigma-Aldrich Corp., St. Louis, MO, USA)). LN229, HepG2, and HuH-7 were maintained in Dulbecco's Modified Eagle Medium (Nacalai Tesque, Inc., Kyoto, Japan). CHO-K1 and P3U1 were maintained in Roswell Park Memorial Institute-1640

 doi:10.20944/preprints202510.2209.v1

medium (Nacalai Tesque, Inc.). These media were supplemented with 100 U/mL penicillin, 100 μg/mL streptomycin, 0.25 μg/mL amphotericin B (Nacalai Tesque, Inc.), and 10% heat-inactivated fetal bovine serum (FBS; Thermo Fisher Scientific, Inc., Waltham, MA, USA). All the cells were cultured in a humidified incubator at 37°C with 5% CO_2.

2.2. Establishment of Stable Transfectants

The expression vector of GPC1 (pCMV6_GPC1, NM_002081) was purchased from OriGene Technologies, Inc. (Rockville, MD, USA). The cDNAs of GPC2 (NM_152742), GPC4 (NM_001448), and GPC5 (NM_004466) were obtained from RIKEN RBC. The cDNAs of GPC3v2 (NM_001164618, designated GPC3) and GPC6 (NM_005708) were synthesized by Eurofins Genomics KK (Tokyo, Japan). The cDNAs of GPC2, GPC3, GPC4, and GPC5 were cloned into a pCAG-ble vector. A GPC6 cDNA was cloned into a pCAGzeo-ssnPA16 vector [41]. The plasmids were transfected into CHO-K1 and LN229 and stable transfectants were established by sorting with an anti-GPC3 mAb (clone SP86; Abcam, Cambridge, UK), an anti-GPC1 mAb (clone 1019718; R&D systems Inc., Minneapolis, MN, USA), an anti-GPC2 mAb (clone CT3; Cell Signaling Technology, Inc., Danvers, MA, USA), an anti-GPC4 mAb (clone A21050B; BioLegend, San Diego, CA, USA), an anti-GPC5 mAb (clone 297716; R&D Systems Inc.), and an anti-PA16 tag mAb (clone NZ-1 for GPC6) [41] using a cell sorter (SH800, Sony Corp., Tokyo, Japan). The GPCs-overexpressed CHO-K1 (e.g., CHO/GPC3) and GPC3-overexpressed LN229 (LN229/GPC3) were finally established.

2.3. Development of Hybridomas

Animal experiments were approved by the Animal Care and Use Committee of Tohoku University (Permit number: 2022MdA-001). They were carried out following the NIH (National Research Council) Guide for the Care and Use of Laboratory Animals. Two female BALB/cAJcl mice (CLEA Japan, Tokyo, Japan) were intraperitoneally immunized with LN229/GPC3 cells (1×10^8 cells/mouse) and Alhydrogel adjuvant 2% (InvivoGen). After three additional immunizations per week (1×10^8 cells/mouse), a booster injection (1×10^8 cells/mouse) was administered 2 days before harvesting spleen cells from immunized mice. The hybridomas were generated as described previously [38]. The supernatants, which were positive for CHO/GPC3 and negative for CHO-K1, were screened by an SA3800 Cell Analyzer (Sony Corporation, Tokyo, Japan).

2.4. Flow Cytometry

Cells were harvested using 1 mM ethylenediaminetetraacetic acid (EDTA; Nacalai Tesque, Inc.). The cells were washed with 0.1% bovine serum albumin (BSA) in phosphate-buffered saline (PBS, blocking buffer) and treated with mAbs for 30 minutes at 4°C. The cells were treated with anti-mouse IgG or anti-rabbit IgG conjugated with Alexa Fluor 488 (2000-fold dilution, Cell Signaling Technology, Inc., Danvers, MA, USA) for 30 minutes at 4°C. The data were collected using an SA3800 Cell Analyzer and analyzed using FlowJo software (BD Biosciences, Franklin Lakes, NJ, USA).

2.5. Determination of Dissociation Constant Values Using Flow Cytometry

CHO/GPC3 and HuH-7 were treated with serially diluted G_3Mab-25. Subsequently, the cells were treated with anti-mouse IgG conjugated with Alexa Fluor 488 (200-fold dilution) for 30 minutes at 4°C. The data were collected using an SA3800 Cell Analyzer and analyzed using FlowJo. The fitting binding isotherms were used to determine the dissociation constant (K_D) values using built-in one-sided binding models in GraphPad Prism 6 (GraphPad Software, Inc., La Jolla, CA, USA).

2.6. Western Blotting

Whole-cell lysates (10 μg of protein) were separated into polyacrylamide gels and transferred onto polyvinylidene difluoride membranes (Merck KGaA, Darmstadt, Germany). The membranes were blocked with 4% skim milk (Nacalai Tesque, Inc.) in PBS containing 0.05% Tween 20 and

 doi:10.20944/preprints202510.2209.v1

incubated with G3Mab-25 (1 μg/mL), SP86 (1 μg/mL), or an anti-isocitrate dehydrogenase 1 (IDH1) mAb (RcMab-1 [42]) (1 μg/mL). Then, the membranes were incubated with anti-mouse IgG conjugated with horseradish peroxidase (for G3Mab-25, Agilent Technologies, Inc., Santa Clara, CA, USA), anti-rabbit IgG conjugated with horseradish peroxidase (for SP86, Agilent Technologies, Inc.), or anti-rat IgG conjugated with horseradish peroxidase (for RcMab-1, Merck KGaA, Darmstadt, Germany). Chemiluminescence signals were developed and detected as described previously [38].

2.7. Immunohistochemistry Using Cell Blocks

Cells were fixed with 4% paraformaldehyde, and the cell blocks were prepared using iPGell (Genostaff Co., Ltd., Tokyo, Japan) (FUJIFILM Wako Pure Chemical Corporation, Osaka, Japan). The formalin-fixed paraffin-embedded (FFPE) cell sections were stained with G3Mab-25 (0.5 μg/mL) or SP86 (0.5 μg/mL) using the ultraView Universal DAB Detection Kit *and BenchMark* ULTRA *PLUS (Roche Diagnostics,* Indianapolis, IN, USA*).*

2.8. Immunohistochemistry Using Tissue Arrays

Solid tumor screen panel (CC00-10-001, Cybrd, Rockville, MD, USA) and liver tumor tissue arrays (BS03013b, T032d, LV242a, and LV243, US Biomax Inc., Rockville, MD, USA) were stained with G3Mab-25 (2 μg/mL) using BenchMark ULTRA PLUS (Roche Diagnostics). Staining intensity, pattern, and cumulative GPC3 expression scores (0-7) were determined as described previously [27,36].

3. Results

3.1. Development of Anti-GPC3 mAbs

To develop anti-GPC3 mAbs, LN229/GPC3 was used as an antigen and immunized in two female BALB/cAJcl mice (Figure 1A). Hybridomas were generated by fusing LN229/GPC3-immunized splenocytes with mouse myeloma P3U1. After forming colonies, the supernatants were screened for CHO/GPC3-positive and CHO-K1-negative (Figure 1B). Subsequently, anti-GPC3 mAb-producing hybridomas were cloned by limiting dilution. We obtained more than 80 anti-GPC3 mAb-producing clones, and their supernatants were further screened for several applications, including western blotting and immunohistochemistry using the CHO/GPC3 block. Finally, a clone, G3Mab-25 (IgG1, κ), was shown to be applicable to these applications (Figure 1C).

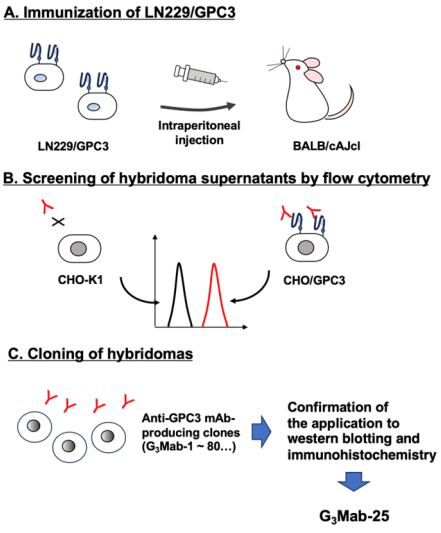

Figure 1. Schematic representation of anti-GPC3 mAbs production. (A) LN229/GPC3 was intraperitoneally immunized in BALB/cAJcl mice (five times). (B) A flow cytometry-based high-throughput screening was

 doi:10.20944/preprints202510.2209.v1

performed to select the CHO/GPC3-positive and CHO-K1-negative supernatants of hybridomas. (C) Anti-GPC3 specific mAb-producing hybridoma clones (more than 80 clones) were established by limiting dilution. After investigation of the applications in western blotting and immunohistochemistry, G3Mab-25 was finally selected.

3.2. Flow Cytometry Using Anti-GPC3 mAbs

We purified G3Mab-25 and performed flow cytometry using G3Mab-25 and a commercially available anti-GPC3 mAb (clone SP86) on CHO/GPC3 and CHO-K1 cells. The G3Mab-25 and SP86 recognized CHO/GPC3 in dose-dependent manner from 10 to 0.01 μg/mL (Figure 2A). Still, they did not recognize CHO-K1 even at 10 μg/mL (Figure 2B). SP86 showed the similar reactivity at 10 and 1 μg/mL but relatively lower reactivity at 0.1 and 0.01 μg/mL compared to G3Mab-25 (Figure 2A). We next investigated the reactivity of G3Mab-25 against an endogenous GPC3-expressing HCC cell lines, HepG2, HuH-7, and JHH-5. G3Mab-25 and SP86 exhibited dose-dependent reactivity of HepG2, HuH-7, and JHH-5 (Figure 3). These results indicate that G3Mab-25 recognizes GPC3 in flow cytometry.

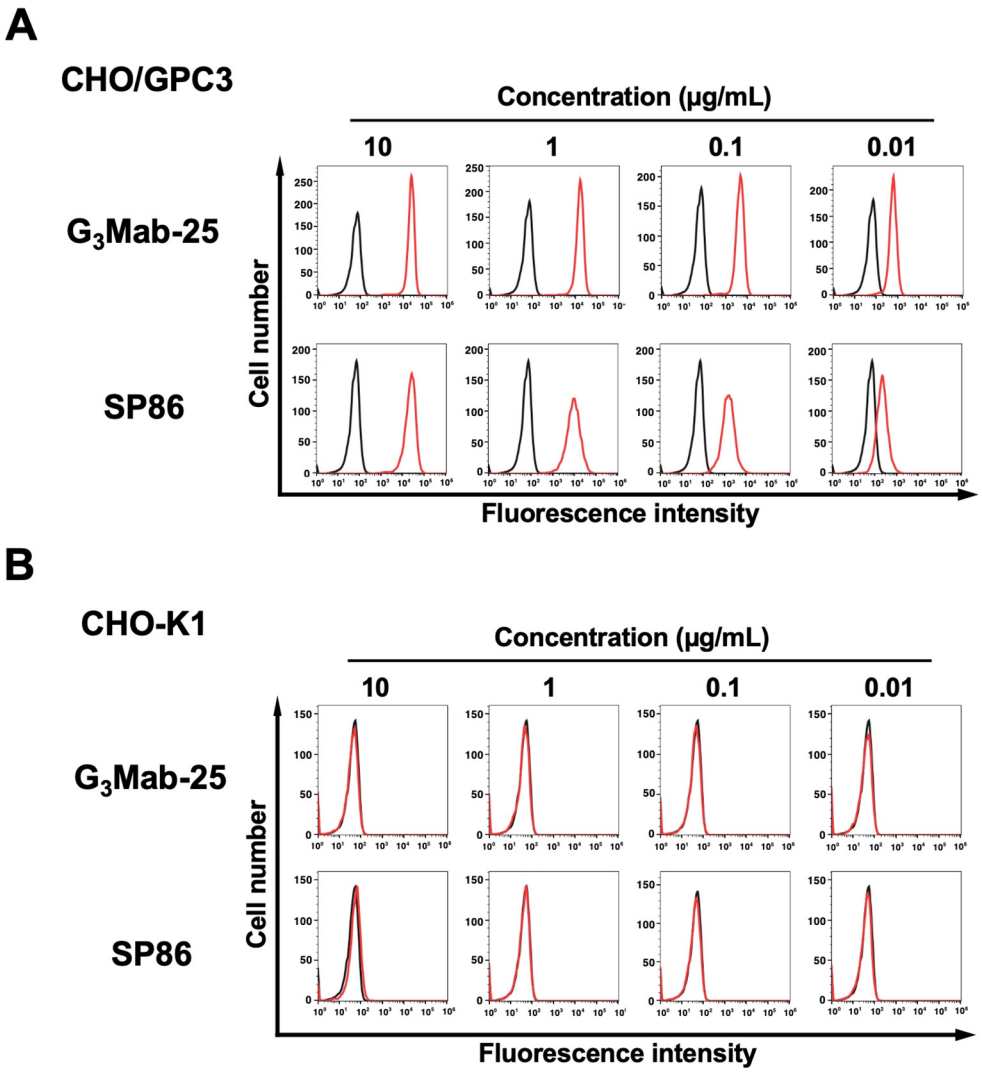

Figure 2. Flow cytometry analysis of G3Mab-25 and SP86 against CHO/GPC3 and CHO-K1. CHO/GPC3 (A) and CHO-K1 (B) were treated with G3Mab-25 or SP86 at the indicated concentrations (red) or blocking buffer (black). The cells were incubated with anti-mouse IgG (for G3Mab-25) or anti-rabbit IgG (for SP86) conjugated with Alexa Fluor 488. The fluorescence data were collected using the SA3800 Cell Analyzer and analyzed using FlowJo.

 doi:10.20944/preprints202510.2209.v1

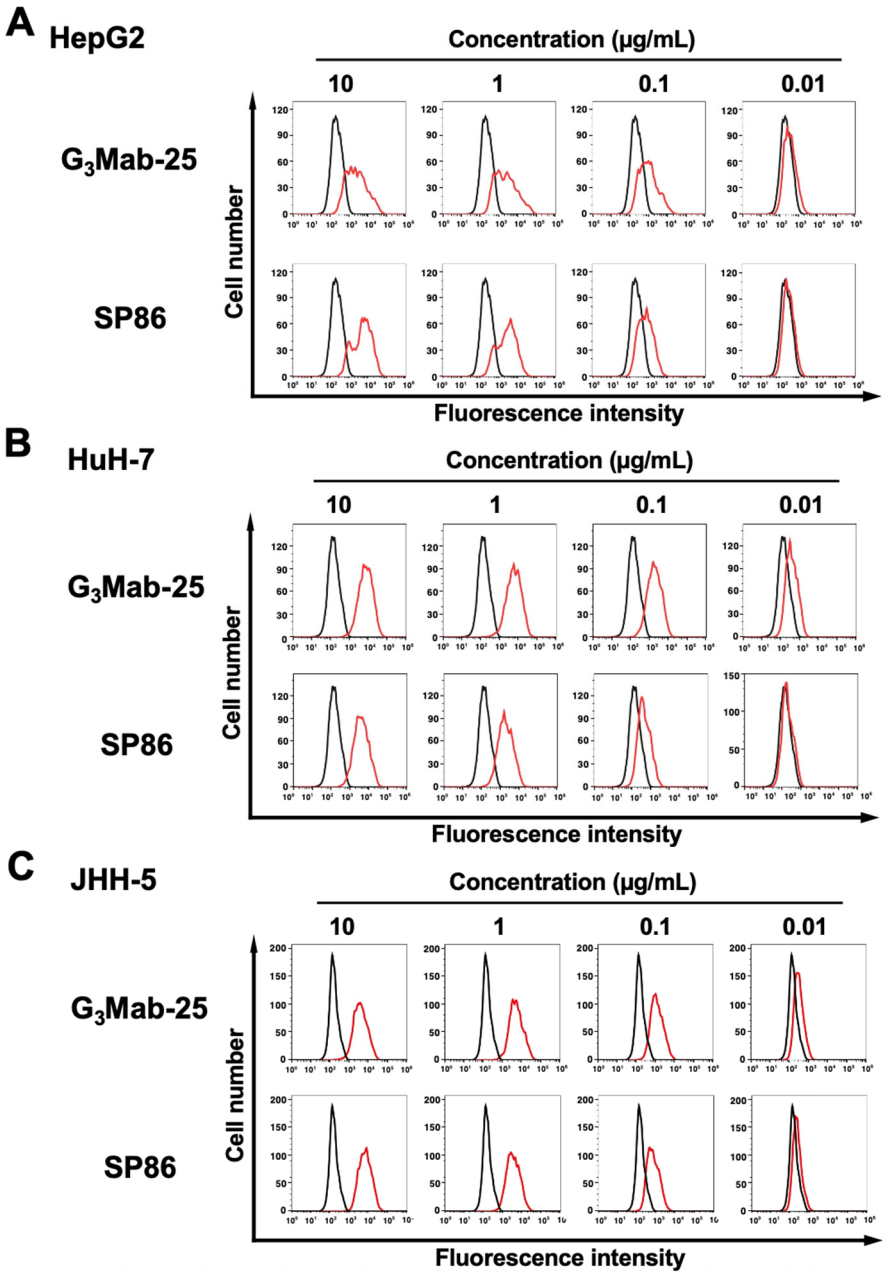

Figure 3. Flow cytometry analysis of G3Mab-25 and SP86 against HCC cell lines. HepG2 (A), HuH-7 (B), and JHH-5 (C) were treated with G3Mab-25 or SP86 at the indicated concentrations (red) or blocking buffer (black). The cells were incubated with anti-mouse IgG (for G3Mab-25) or anti-rabbit IgG (for SP86) conjugated with Alexa Fluor 488. The fluorescence data were collected using the SA3800 Cell Analyzer and analyzed using FlowJo.

3.3. Specificity of G3Mab-25 Against GPC Family Members

Using GPC1 ~ GPC 6-overexpressed CHO-K1, the specificity of G3Mab-25 was investigated. As shown in Figure 4, G3Mab-25 recognized CHO/GPC3 and did not react with other GPC-overexpressed CHO-K1. These results indicate that G3Mab-25 is a specific mAb against GPC3 within the GPC family.

 doi:10.20944/preprints202510.2209.v1

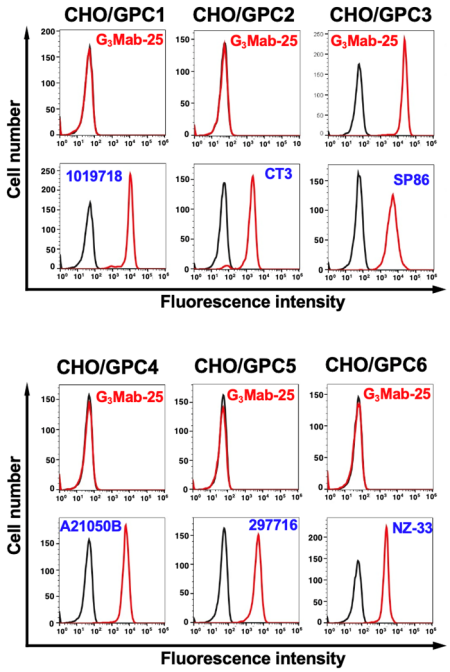

Figure 4. Flow cytometry analysis of G3Mab-25 in GPC family members-overexpressed CHO-K1. The GPC family members (GPC1, GPC2, GPC3, GPC4, GPC5, and PA16-GPC6)-overexpressed CHO-K1 were treated with 1 μg/mL of G3Mab-25 (red) or control blocking buffer (black). The expression of each GPC was confirmed by 1 μg/mL of an anti-GPC3 mAb (clone 1019718), 1 μg/mL of an anti-GPC2 mAb (clone CT3), 1 μg/mL of an anti-GPC3 mAb (clone SP86), 1 μg/mL of an anti-GPC4 mAb (clone A21050B), 1 μg/mL of an anti-GPC5 mAb (clone 297716), and 1 μg/mL of an anti-PA16 mAb, NZ-1. Then, the cells were incubated with anti-mouse IgG, anti-rabbit IgG (for SP86), or anti-rat IgG (for NZ-1) conjugated with Alexa Fluor 488. The fluorescence data were collected using the SA3800 Cell Analyzer and analyzed using FlowJo.

3.4. Determination of KD Values of G3Mab-25 by Flow Cytometry

The binding affinity of G3Mab-25 was determined using a flow cytometry-based approach. The *K*D values of G3Mab-25 for CHO/GPC3 and HuH-7 were 1.8 × 10^{-8} M and 3.9 × 10^{-9} M, respectively (Figure 5). The *K*D values of SP86 for CHO/GPC3 could not be determined because the sigmoid curve did not reach a plateau (Supplementary Figure S1). These results indicated that G3Mab-25 has high affinity to GPC3-positive cells.

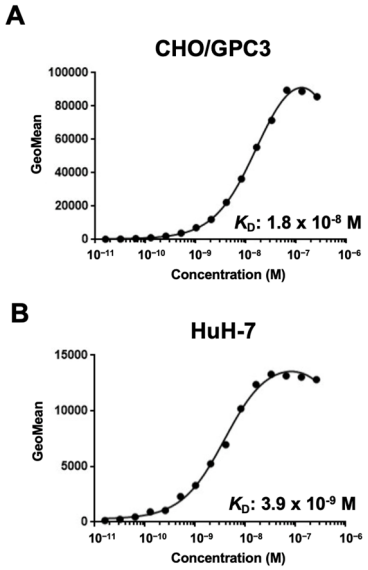

 doi:10.20944/preprints202510.2209.v1

Figure 5. Measurement of Binding affinity of G3Mab-25 using flow cytometry. CHO/GPC3 was treated with serially diluted G3Mab-25 followed by anti-mouse IgG conjugated with Alexa Fluor 488. The fluorescence data were analyzed using the SA3800 Cell Analyzer. The K_D values were determined using GraphPad PRISM 6.

3.5. Western Blotting Using Anti-GPC3 mAbs

We next performed western blotting using G3Mab-25 and SP86. Whole-cell lysates of CHO-K1, CHO/GPC3, HepG2, HuH-7, and JHH-5 were used. G3Mab-25 detected 70-kDa and 40-kDa bands in CHO/GPC3, HepG2, HuH-7, and JHH-5, but not in CHO-K1 (Figure 6A). SP86 detected 70-kDa and 17-kDa bands in CHO/GPC3 in CHO/GPC3 (Figure 6B). Although SP86 detected 70-kDa band in HepG2, it was not detected in HuH-7 and JHH-5 (Figure 6B). Furthermore, the 17-kDa band was weak in HepG2 and was not detected in HuH-7 and JHH-5 (Figure 6B). IDH1 detected by RcMab-1 was used as an internal control (Figure 6C). Figure 6D represents the structure of GPC3. These results indicated that G3Mab-25 detected the 70-kDa (uncleaved form) and N-terminal fragment (40 kDa) of GPC3. In contrast, SP86 detected the 70-kDa (uncleaved form) and C-terminal fragment (17 kDa) of GPC3.

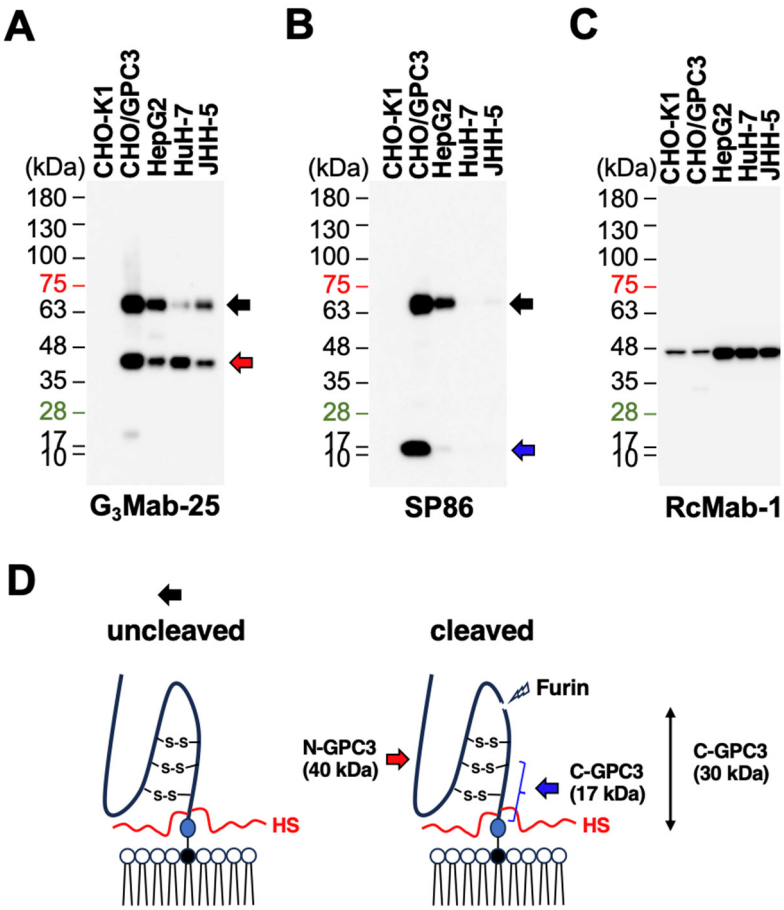

Figure 6. Western blotting using anti-GPC3 mAbs. The cell lysates of CHO-K1, CHO/GPC3, HepG2, HuH-7, and JHH-5 were electrophoresed and transferred onto polyvinylidene difluoride membranes. The membranes were incubated with 1 μg/mL of G3Mab-25 (A), 1 μg/mL of SP86 (B), or 1 μg/mL of RcMab-1 (an anti-IDH1 mAb, C), followed by treatment with anti-mouse (for G3Mab-25), anti-rabbit (for SP86), or anti-rat IgG (for RcMab-1) conjugated with horseradish peroxidase. Note that the exposure time of A and B was same. Black arrow represents uncleaved form of GPC3. Red arrow represents N-terminal fragment of GPC3 (N-GPC3). Blue arrow represents C-terminal fragment of GPC3 (C-GPC3). (D) Schematic representation of uncleaved and cleaved forms of GPC3.

 doi:10.20944/preprints202510.2209.v1

3.6. Immunohistochemistry Using Cell Blocks

We next performed IHC in FFPE sections of CHO-K1 and CHO/GPC3 using G3Mab-25 and SP86 with BenchMark ULTRA PLUS, a fully automated slide staining system. Both membranous and cytoplasmic staining were detected in CHO/GPC3 but not in CHO-K1 by G3Mab-25 and SP86 (Figure 7). These results indicated that G3Mab-25 and SP86 can detect GPC3 in FFPE cell sections.

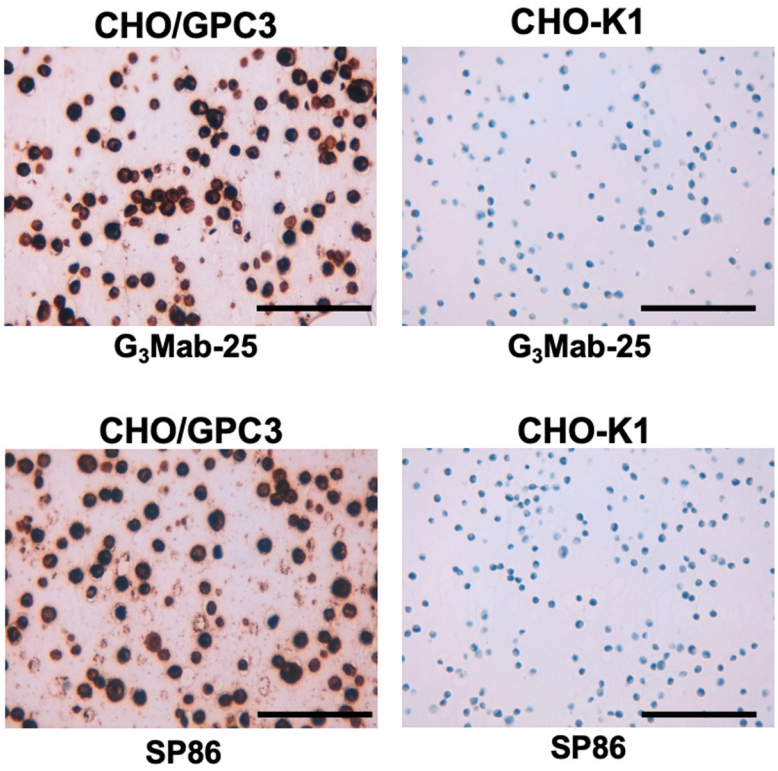

Figure 7. Immunohistochemistry using G3Mab-25 in formalin-fixed paraffin-embedded cell blocks. CHO/GPC3 and CHO-K1 sections were treated with 1 μg/mL of G3Mab-25 (A) or 1 μg/mL of SP86 (B). The staining was performed using ultraView Universal DAB Detection Kit *and BenchMark* ULTRA *PLUS*. Scale bar = 100 μm.

3.7. Immunohistochemistry Using Cell Blocks

Since GPC3 is frequently overexpressed in HCC, we next investigated whether G3Mab-25 could detect GPC3 in a tissue array from a solid tumor screening panel. As summarized in Supplementary Figure S2 and Table S1, G3Mab-25 showed the cytoplasmic granular staining (score 1) in HCC sections, but not in other tumor sections. We further stained the liver tumor tissue arrays in the same experimental setting. As shown in Figure 8, an intense diffuse cytoplasmic/membranous staining (score 7), cytoplasmic granular/moderate membranous staining (score 5), and weak membranous staining (score 3) were also observed. Furthermore, the negative staining (score 0) was also observed in some cases of HCC and normal liver. Supplementary Table S2 summarizes the results. These results indicated that G3Mab-25 exhibited the diverse staining pattern of GPC3 in HCC tissues.

 doi:10.20944/preprints202510.2209.v1

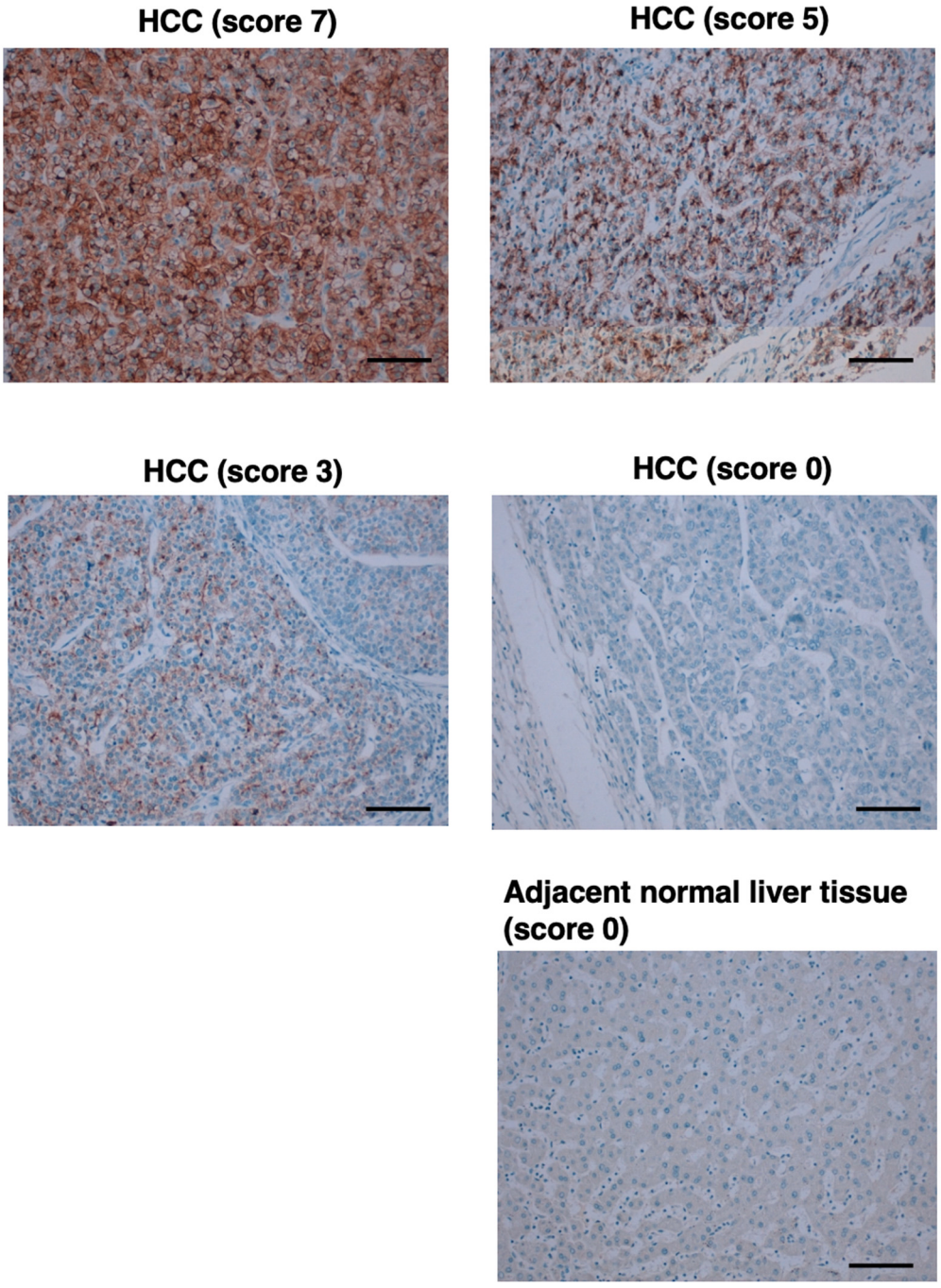

Figure 8. Immunohistochemistry using G3Mab-25 in liver tumor tissue arrays. Liver tumor tissue arrays were treated with 2 μg/mL of G3Mab-25. The staining was performed using ultraView Universal DAB Detection Kit *and BenchMark* ULTRA *PLUS*. Strong membranous staining (score 7), moderate membranous staining (score 5), weak membranous staining (score 3), and no staining (score 0) were shown. Scale bar = 100 μm.

4. Discussion

We have established more than 80 clones of anti-GPC3 mAbs by the CBIS method and updated the information on our website "Antibody bank (http://www.med-tohoku-antibody.com/topics/001_paper_antibody_PDIS.htm)". Among them, G3Mab-25 exhibited the reactivity to exogenous and endogenous GPC3 (Figure 2 and 3) and superior affinity (Figure 5 and Supplemental Figure S1) compared to SP86, a commercially available anti-GPC3 mAb. G3Mab-25 showed the specificity to GPC3 among GPC family members (Figure 4). Furthermore, G3Mab-25 can detect the N-terminal fragment of GPC3 in western blotting (Figure 6) and membranous and

 doi:10.20944/preprints202510.2209.v1

cytoplasmic GPC3 in IHC (Figure 7 and 8). Therefore, G3Mab-25 possesses high versatility for basic research and could be applied to tumor diagnosis and therapy.

Wnt signaling is a central regulator of HCC progression [43]. In addition to the canonical receptor Frizzled (FZD), multiple coreceptors, including HS proteoglycans, participate in Wnt signaling activation. GPC3 serves as a Wnt coreceptor promoting HCC cell proliferation through recruitment of Wnt ligands to the C-terminal HS [44]. Furthermore, a structural model of GPC3-Wnt complex revealed that a Wnt-binding groove located in the putative FZD-like cysteine-rich domain at the N-terminal domain of GPC3 [45]. The GPC3 groove around residue Phe41 interacts with the middle region of Wnt3a. Mutations within this groove markedly reduced Wnt3a binding, β-catenin activation, and inhibited HCC tumor growth in mice [45]. Significantly, blockade of this domain with a specific antibody against the N-terminal domain of GPC3 suppressed Wnt activation [45], suggesting a potential therapeutic site on GPC3 for Wnt inhibition and HCC treatment. Since G3Mab-25 recognizes the N-terminal fragment of GPC3 in western blotting (Figure 6), epitope mapping and the inhibitory effect on Wnt signaling should be investigated in the future.

G3Mab-25 clearly recognizes the endogenous N-terminal 40-kDa fragment of GPC3 (Figure 6A). In contrast, SP86 recognizes the endogenous C-terminal 17-kDa fragment of GPC3, but the reactivity is low (Figure 6B), suggesting the low stability of the C-terminal 17-kDa fragment. More prolonged exposure of the western blot membrane showed the endogenous C-terminal 17-kDa fragment in HCC cell lines (Supplementary Figure S3A). Additionally, we obtained G3Mab-49 and G3Mab-52, which also recognize the C-terminal 17-kDa fragment (Supplementary Figure S3B). A similar result was reported by another group [46]. After Furin cleavage of GPC3, the C-terminal fragment possesses about 200 amino acids, and the estimated molecular weight is 30 kDa [17,29]. Since these mAbs can detect membrane-bound GPC3 in flow cytometry, they probably recognize a juxtamembrane C-terminal region of GPC3 (Figure 6D). It should be determined whether the C-terminal 30-kDa fragment is further processed to a 17-kDa fragment or not.

Immunohistochemistry is an essential technique for tumor diagnosis. Clinically, BenchMark ULTRA PLUS is used for the diagnosis of HER2-positive tumors, which determines the application of anti-HER2 therapies [47]. For the use of trastuzumab in patients with breast cancer, HER2-overexpression should be determined by intense and complete membranous staining of more than 10% of cells in immunohistochemistry (IHC 3+) [48]. The GPC3 overexpression was evaluated in the different scoring in clinical trials [27,36,49]. This study follows a scoring system as recently used in a clinical trial [36]. Therefore, standardization of IHC is essential for patient selection. Since G3Mab-25 works within the standard staining protocol of BenchMark ULTRA PLUS (Figure 7 and Figure 8), It would contribute to standardizing HCC diagnosis.

An anti-GPC3 mAb clone GC33 (mouse IgG_{2a}, κ) was established by the immunization of bacterially-expressed C-terminal fragment (amino acids 524–563) of GPC3 [23]. GC33 exhibited high binding affinity, ADCC, and antitumor efficacy in preclinical study [25]. However, the humanized mAb, codrituzumab, failed to improve survival in clinical studies [29]. Codrituzumab may exhibit limited efficacy due to glycosylation-related modifications that affect antibody binding. Glycosylation of antigens, including PD-1 and PD-L1, has been reported to mask binding epitopes and diminish therapeutic activity [50]. Similarly, glycosylation near the C-terminal region or HS modification of GPC3 may limit antibody accessibility. Our anti-GPC3 mAbs established by the CBIS method recognize a variety of epitopes, including conformational epitopes, linear epitopes, and glyco-epitopes, which enable the selection of antitumor efficacy *in vivo*. We have initiated cloning of cDNA from anti-GPC3 mAb clones, including G3Mab-25, and will evaluate ADCC and antitumor efficacy using class-switched (mouse IgG_{2a} or human IgG_1) mAbs.

In the development of CAR-T, the property of single-chain variable fragment, including binding affinity and epitope, determines the persistence, tonic signaling, exhaustion, and therapeutic efficacy [51]. Although a variety of CAR against CD19 has been evaluated in the clinic [52], the variation of anti-GPC3 CAR is still limited. G3Mabs will enable optimization of anti-GPC3 CAR-T cell therapy.

 doi:10.20944/preprints202510.2209.v1

Supplementary Materials: The following supporting information can be downloaded at the website of this paper posted on Preprints.org.

Credit: authorship contribution statement. Saori Okuno: Investigation. **Hiroyuki Suzuki:** Investigation, Writing – original draft. **Mika K. Kaneko:** Conceptualization. **Yukinari Kato:** Conceptualization, Funding acquisition, Project administration, Writing – review and editing. **All:** authors have read and agreed to the published version of the manuscript.

Funding Information: This research was supported in part by Japan Agency for Medical Research and Development (AMED) under Grant Numbers: JP25am0521010 (to Y.K.), JP25ama121008 (to Y.K.), JP25ama221339 (to Y.K.), and JP25bm1123027 (to Y.K.), and by the Japan Society for the Promotion of Science (JSPS) Grants-in-Aid for Scientific Research (KAKENHI) grant no. 25K10553 (to Y.K.).
Institutional Review Board Statement: The animal study protocol was approved by the Animal Care and Use Committee of Tohoku University (Permit number: 2022MdA-001) for studies involving animals.

Informed Consent Statement: Not applicable.

Data Availability Statement: All related data and methods are presented in this paper. Additional inquiries should be addressed to the corresponding authors.
Conflicts of Interest: The authors declare no conflict of interest involving this article.

References

1. Fico, A.; Maina, F.; Dono, R. Fine-tuning of cell signaling by glypicans. *Cell Mol Life Sci* 2011;*68*(6): 923-929.
2. Filmus, J.; Capurro, M. The role of glypicans in Hedgehog signaling. *Matrix Biol* 2014;*35*: 248-252.
3. Kolluri, A.; Ho, M. The Role of Glypican-3 in Regulating Wnt, YAP, and Hedgehog in Liver Cancer. *Front Oncol* 2019;*9*: 708.
4. De Cat, B.; Muyldermans, S.Y.; Coomans, C.; et al. Processing by proprotein convertases is required for glypican-3 modulation of cell survival, Wnt signaling, and gastrulation movements. *J Cell Biol* 2003;*163*(3): 625-635.
5. Piao, Q.; Bian, X.; Zhao, Q.; Sun, L. Unraveling Glypican-3: From Structural to Pathophysiological Roles and Mechanisms-An Integrative Perspective. *Cells* 2025;*14*(10).
6. Song, H.H.; Filmus, J. The role of glypicans in mammalian development. *Biochim Biophys Acta* 2002;*1573*(3): 241-246.
7. Watanabe, K.; Yamada, H.; Yamaguchi, Y. K-glypican: a novel GPI-anchored heparan sulfate proteoglycan that is highly expressed in developing brain and kidney. *J Cell Biol* 1995;*130*(5): 1207-1218.
8. Baumhoer, D.; Tornillo, L.; Stadlmann, S.; et al. Glypican 3 expression in human nonneoplastic, preneoplastic, and neoplastic tissues: a tissue microarray analysis of 4,387 tissue samples. *Am J Clin Pathol* 2008;*129*(6): 899-906.
9. Song, H.H.; Shi, W.; Xiang, Y.Y.; Filmus, J. The loss of glypican-3 induces alterations in Wnt signaling. *J Biol Chem* 2005;*280*(3): 2116-2125.
10. Capurro, M.I.; Xu, P.; Shi, W.; et al. Glypican-3 inhibits Hedgehog signaling during development by competing with patched for Hedgehog binding. *Dev Cell* 2008;*14*(5): 700-711.
11. Lum, L.; Yao, S.; Mozer, B.; et al. Identification of Hedgehog pathway components by RNAi in Drosophila cultured cells. *Science* 2003;*299*(5615): 2039-2045.
12. Topczewski, J.; Sepich, D.S.; Myers, D.C.; et al. The zebrafish glypican knypek controls cell polarity during gastrulation movements of convergent extension. *Dev Cell* 2001;*1*(2): 251-264.
13. Perrimon, N.; Bernfield, M. Specificities of heparan sulphate proteoglycans in developmental processes. *Nature* 2000;*404*(6779): 725-728.
14. Baeg, G.H.; Perrimon, N. Functional binding of secreted molecules to heparan sulfate proteoglycans in Drosophila. *Curr Opin Cell Biol* 2000;*12*(5): 575-580.
15. Bhave, V.S.; Mars, W.; Donthamsetty, S.; et al. Regulation of liver growth by glypican 3, CD81, hedgehog, and Hhex. *Am J Pathol* 2013;*183*(1): 153-159.
16. Ochoa, B.; Syn, W.K.; Delgado, I.; et al. Hedgehog signaling is critical for normal liver regeneration after partial hepatectomy in mice. *Hepatology* 2010;*51*(5): 1712-1723.

 doi:10.20944/preprints202510.2209.v1

17. Schepers, E.J.; Glaser, K.; Zwolshen, H.M.; Hartman, S.J.; Bondoc, A.J. Structural and Functional Impact of Posttranslational Modification of Glypican-3 on Liver Carcinogenesis. *Cancer Res* 2023;*83*(12): 1933-1940.
18. Hippo, Y.; Watanabe, K.; Watanabe, A.; et al. Identification of soluble NH2-terminal fragment of glypican-3 as a serological marker for early-stage hepatocellular carcinoma. *Cancer Res* 2004;*64*(7): 2418-2423.
19. Nakatsura, T.; Yoshitake, Y.; Senju, S.; et al. Glypican-3, overexpressed specifically in human hepatocellular carcinoma, is a novel tumor marker. *Biochem Biophys Res Commun* 2003;*306*(1): 16-25.
20. Capurro, M.; Wanless, I.R.; Sherman, M.; et al. Glypican-3: a novel serum and histochemical marker for hepatocellular carcinoma. *Gastroenterology* 2003;*125*(1): 89-97.
21. Lin, Y.; Ma, Y.; Chen, Y.; et al. Diagnostic and prognostic performance of serum GPC3 and PIVKA-II in AFP-negative hepatocellular carcinoma and establishment of nomogram prediction models. *BMC Cancer* 2025;*25*(1): 721.
22. Devan, A.R.; Nair, B.; Pradeep, G.K.; et al. The role of glypican-3 in hepatocellular carcinoma: Insights into diagnosis and therapeutic potential. *Eur J Med Res* 2024;*29*(1): 490.
23. Nakano, K.; Orita, T.; Nezu, J.; et al. Anti-glypican 3 antibodies cause ADCC against human hepatocellular carcinoma cells. *Biochem Biophys Res Commun* 2009;*378*(2): 279-284.
24. Feng, M.; Ho, M. Glypican-3 antibodies: a new therapeutic target for liver cancer. *FEBS Lett* 2014;*588*(2): 377-382.
25. Ishiguro, T.; Sugimoto, M.; Kinoshita, Y.; et al. Anti-glypican 3 antibody as a potential antitumor agent for human liver cancer. *Cancer Res* 2008;*68*(23): 9832-9838.
26. Abou-Alfa, G.K.; Puig, O.; Daniele, B.; et al. Randomized phase II placebo controlled study of codrituzumab in previously treated patients with advanced hepatocellular carcinoma. *J Hepatol* 2016;*65*(2): 289-295.
27. Zhu, A.X.; Gold, P.J.; El-Khoueiry, A.B.; et al. First-in-man phase I study of GC33, a novel recombinant humanized antibody against glypican-3, in patients with advanced hepatocellular carcinoma. *Clin Cancer Res* 2013;*19*(4): 920-928.
28. Tsuchiya, N.; Hosono, A.; Yoshikawa, T.; et al. Phase I study of glypican-3-derived peptide vaccine therapy for patients with refractory pediatric solid tumors. *Oncoimmunology* 2017;*7*(1): e1377872.
29. Zhang, J.; Li, R.; Tan, X.; Wang, C. Targeting Glypican-3 for Liver Cancer Therapy: Clinical Applications and Detection Methods. *J Clin Transl Hepatol* 2025;*13*(8): 665-681.
30. Filippi, L.; Frantellizzi, V.; Urso, L.; De Vincentis, G.; Urbano, N. Targeting Glypican-3 in Liver Cancer: Groundbreaking Preclinical and Clinical Insights. *Biomedicines* 2025;*13*(7).
31. Carrasquillo, J.A.; O'Donoghue, J.A.; Beylergil, V.; et al. I-124 codrituzumab imaging and biodistribution in patients with hepatocellular carcinoma. *EJNMMI Res* 2018;*8*(1): 20.
32. Bell, M.M.; Gutsche, N.T.; King, A.P.; et al. Glypican-3-Targeted Alpha Particle Therapy for Hepatocellular Carcinoma. *Molecules* 2020;*26*(1).
33. Zhou, Y.; Wei, S.; Xu, M.; et al. CAR-T cell therapy for hepatocellular carcinoma: current trends and challenges. *Front Immunol* 2024;*15*: 1489649.
34. Li, J.; Liu, C.; Zhang, P.; Shen, L.; Qi, C. Optimizing CAR T cell therapy for solid tumours: a clinical perspective. *Nat Rev Clin Oncol* 2025.
35. Yong, C.S.M.; Dardalhon, V.; Devaud, C.; et al. CAR T-cell therapy of solid tumors. *Immunol Cell Biol* 2017;*95*(4): 356-363.
36. Steffin, D.; Ghatwai, N.; Montalbano, A.; et al. Interleukin-15-armoured GPC3 CAR T cells for patients with solid cancers. *Nature* 2025;*637*(8047): 940-946.
37. Ubukata, R.; Ohishi, T.; Kaneko, M.K.; Suzuki, H.; Kato, Y. EphB2-Targeting Monoclonal Antibodies Exerted Antitumor Activities in Triple-Negative Breast Cancer and Lung Mesothelioma Xenograft Models. *Int J Mol Sci* 2025;*26*(17).
38. Satofuka, H.; Suzuki, H.; Tanaka, T.; et al. Development of an anti-human EphA2 monoclonal antibody Ea(2)Mab-7 for multiple applications. *Biochem Biophys Rep* 2025;*42*: 101998.
39. Suzuki, H.; Tanaka, T.; Li, G.; et al. Development of a Sensitive Anti-Mouse CCR5 Monoclonal Antibody for Flow Cytometry. *Monoclon Antib Immunodiagn Immunother* 2024;*43*(4): 96-100.
40. Nanamiya, R.; Takei, J.; Asano, T.; et al. Development of Anti-Human CC Chemokine Receptor 9 Monoclonal Antibodies for Flow Cytometry. *Monoclon Antib Immunodiagn Immunother* 2021;*40*(3): 101-106.

 doi:10.20944/preprints202510.2209.v1

41. Fujii, Y.; Kaneko, M.; Neyazaki, M.; et al. PA tag: a versatile protein tagging system using a super high affinity antibody against a dodecapeptide derived from human podoplanin. *Protein Expr Purif* 2014;*95*: 240-247.
42. Ikota, H.; Nobusawa, S.; Arai, H.; et al. Evaluation of IDH1 status in diffusely infiltrating gliomas by immunohistochemistry using anti-mutant and wild type IDH1 antibodies. *Brain Tumor Pathol* 2015;*32*(4): 237-244.
43. Lehrich, B.M.; Monga, S.P. WNT-β-catenin signalling in hepatocellular carcinoma: from bench to clinical trials. *Nat Rev Gastroenterol Hepatol* 2025.
44. Gao, W.; Xu, Y.; Liu, J.; Ho, M. Epitope mapping by a Wnt-blocking antibody: evidence of the Wnt binding domain in heparan sulfate. *Sci Rep* 2016;*6*: 26245.
45. Li, N.; Wei, L.; Liu, X.; et al. A Frizzled-Like Cysteine-Rich Domain in Glypican-3 Mediates Wnt Binding and Regulates Hepatocellular Carcinoma Tumor Growth in Mice. *Hepatology* 2019;*70*(4): 1231-1245.
46. Yamauchi, N.; Watanabe, A.; Hishinuma, M.; et al. The glypican 3 oncofetal protein is a promising diagnostic marker for hepatocellular carcinoma. *Mod Pathol* 2005;*18*(12): 1591-1598.
47. Robbins, C.J.; Bates, K.M.; Rimm, D.L. HER2 testing: evolution and update for a companion diagnostic assay. *Nat Rev Clin Oncol* 2025;*22*(6): 408-423.
48. Cardoso, F.; Paluch-Shimon, S.; Senkus, E.; et al. 5th ESO-ESMO international consensus guidelines for advanced breast cancer (ABC 5). *Ann Oncol* 2020;*31*(12): 1623-1649.
49. Li, B.; Huang, L.; Huang, J.; Li, J. An Update of Immunohistochemistry in Hepatocellular Carcinoma. *Diagnostics (Basel)* 2025;*15*(17).
50. Lee, H.H.; Wang, Y.N.; Xia, W.; et al. Removal of N-Linked Glycosylation Enhances PD-L1 Detection and Predicts Anti-PD-1/PD-L1 Therapeutic Efficacy. *Cancer Cell* 2019;*36*(2): 168-178.e164.
51. Nguyen, T.T.; Ho, P.; Staudt, S.; et al. Fine tuning towards the next generation of engineered T cells. *Nat Biomed Eng* 2025;*9*(10): 1610-1631.
52. Ben Valid, O.; Shouval, R. Predictors of response to CD19 chimeric antigen receptor T-cell therapy in large B-cell lymphoma: a consolidated review. *Curr Opin Oncol* 2025;*37*(6): 625-632.